

An optimal design of thermal protection based on materials morphology

Margarita O. Salosina, Oleg M. Alifanov, Aleksey V. Nenarokomov
Moscow Aviation Institute
4 Volokolamskoe Hgw., Moscow, 125993, Russia
e-mail: salosina.m@yandex.ru

The paper presents a methodology for the optimal design of multilayer thermal protection based on high-porosity open-cell foam, taking into account the foam morphology. The vector of design parameters includes the thicknesses of layers, porosity and cell diameter of open-cell foam and should ensure required operation temperature on the boundaries of layers and a minimum of the total mass of the system. The optimization problem is solved using a computational scheme, which combines the projected Lagrangian method with the quadratic subproblem and the penalty function method. The penalty function method provides a good initial estimate of the optimal parameters' values for the projected Lagrangian method with excellent local convergence properties. To illustrate the implementation of the developed algorithm and the corresponding software, the problem of choosing the optimal layer thicknesses for the multilayer thermal protection of a spacecraft along with the cell diameter and porosity of foam is considered.

Keywords: optimal design, multilayer thermal protection, open-cell foam.

NOMENCLATURE

\mathbf{A}	–	Jacobian matrix of constraints,
B	–	parameter characterized a boundary condition,
F	–	parameter characterized a boundary condition,
b_{\min}	–	minimum strut diameter,
b_{\max}	–	maximum strut diameter,
C	–	volumetric heat capacity,
c_s	–	specific heat capacity of the solid phase,
d_l	–	layer thickness,
a	–	cell diameter,
ε	–	emissivity,
\mathbf{H}	–	Hessian matrix,
I	–	radiative emissive power,
J	–	minimized function,
k_R	–	radiative conductivity,
L	–	number of layers in system,
N	–	number of desired parameters,
$N\tau$	–	number of steps by time,
\mathbf{p}	–	vector of parameters,

q	– heat flux,
R	– contact thermal resistance,
r	– solid surface reflectivity,
\mathbf{s}	– search direction,
T	– temperature,
T_{lim}^l	– temperature constraint at the boundary of layer,
X	– coordinate of layer boundary,
α	– absorption coefficient,
β	– extinction coefficient,
β_R^*	– Rosseland mean extinction coefficient,
γ	– step length,
δ	– porosity,
λ_l	– thermal conductivity,
λ_n	– thermal conductivity in the absence of radiation,
λ_s	– thermal conductivity of solid phase,
ρ	– density,
σ	– scattering coefficient,
k_B	– Boltzmann constant,
τ	– time,
$\Phi(\theta)$	– scattering phase function,
$\boldsymbol{\psi}^T$	– vector of Lagrange multiplier,
ω	– scattering albedo.

Subscripts

b	– blackbody,
R	– radiative,
s	– solid phase,
λ	– wavelength.

1. INTRODUCTION

During the operation, structures and systems of solar and planetary probes are subjected to extreme heat loads. The design of reliable and efficient thermal protection of such space vehicles is very critical because its failure leads to catastrophic consequences for the whole mission.

Often the successful fulfillment of the mission's scientific goals greatly depends on the practical solution of problems related to the choice of the thermal protection concept and high-temperature heat-resistant construction materials. The relative weight of the space vehicle thermal protection remains significant, thus making the problem of increasing its weight efficiency actual.

The most promising way to solve this problem is to use light heat-shielding and heat-insulating materials. Highly porous cellular materials have great potential for manufacturing of high-temperature thermal insulation. The benefits of such materials include extremely low density, high-temperature capability, sufficient strength at the operating temperatures, and low thermal conductivity.

Highly porous cellular materials are fabricated by applying a layer of inorganic material (metals, oxides, carbides, etc.) to the surface of a highly porous open-cell organic matrix, for example, polyurethane foam, and subsequently removing the structure-forming matrix by thermal destruc-

tion in a special medium. The manufacturing technology of open-cell carbon foam is based on the pyrolysis of polyurethane foam, previously impregnated with phenol-formaldehyde resin.

Open-cell carbon foam can serve as the basis for the production of composite materials with unique thermal, mechanical, spectral and chemical properties. These materials are obtained by infiltration of graphite, refractory metals (niobium, tantalum, tungsten, molybdenum, rhenium) or ceramics (oxides, nitrides, carbides, borides and silicides of any metal) into the carbon foam.

The open-cell foams are characterized by high homogeneity of the structure and a small deviation of the cell sizes from the mean value. The structure of open-cell carbon foam consists of an interconnected network of solid struts (see Fig. 1). The unit cell appears to closely resemble a pentagon dodecaeder with twelve pentagonal faces. Sometimes the unit cell is also presented as a cube or a 14-faceted tetrakaidecahedron. In common foams, four struts are connected, making a strut juncture. From microscope analysis, it can be observed that the struts have varying thickness, and the cross-section of struts formed at the junction of three cells is concave, triangularly incurved. Namely, it seems to be inscribed in an equilateral triangle (see Fig. 2). Along with the pentagonal faces, tetragonal and hexagonal faces are found in the structure of the material. In addition, there is anisotropy of cell sizes associated with the foaming process. However, despite the noted deviations in the morphology of cells, the materials are assumed to be identical in all three directions.

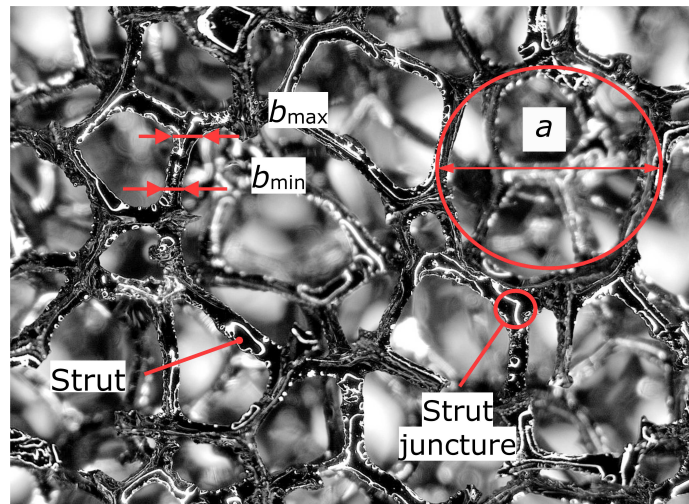


Fig. 1. Structure parameters of open-cell foam.

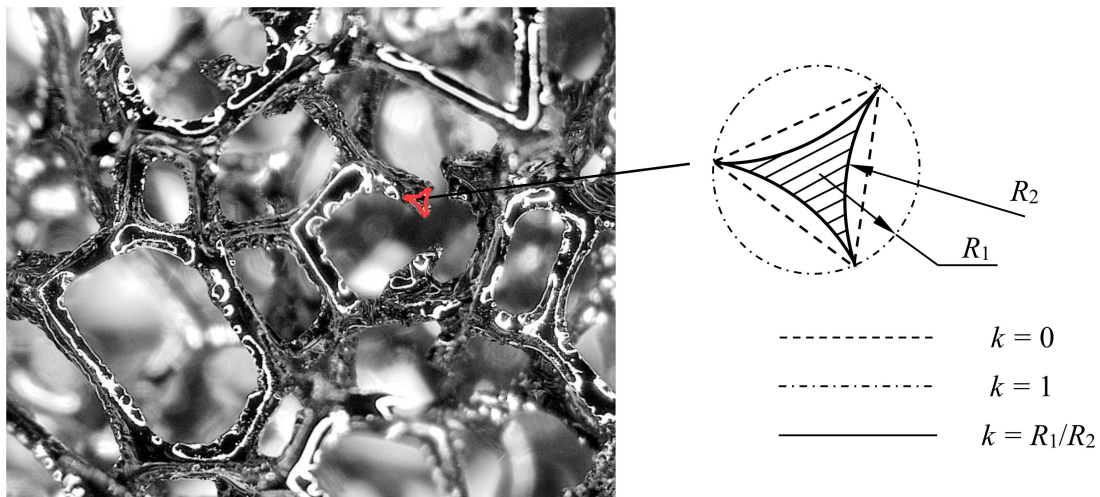


Fig. 2. Strut cross-section's shape.

The main parameters of open-cell carbon foams describing the structure of the material are the average cell size and the porosity characterizing the space inside the cells. The size of the cell determines the length and number of struts per unit volume of material, and the porosity controls the cross-section shape and actual size of struts and strut junctions.

Physical properties of cellular materials are not only determined by their base material but also significantly by their microstructure (cell dimensions, length and cross-sectional dimensions of the struts), the technology of fabrication, and operating conditions. This implies the possibility to create open-cell materials with desirable properties, optimal for specific applications.

The design parameters describing the structure of highly porous cellular materials should have a great influence on the radiation properties of the material, be easily measured using the available means for image processing of the samples' microstructure and controlled during the manufacturing process of the material.

Theoretical results obtained using Monte Carlo methods show that porosity and average cell diameter have the greatest effects on the radiation properties of open-cell foams [6]. Variations of strut diameter along the length and strut's cross-section shape have moderate effects on the extinction coefficient of the porous medium. Dispersion of cell size from the average value does not have a noticeable effect on the radiation properties of the material [6]. Thus, the porosity and cell diameter of open-cell foam can be considered as the design parameters, characterizing the structure of highly porous cellular materials.

This paper presents a methodology for the optimal design of multilayer thermal insulation based on high-porosity open-cell foam, taking into account the dependence of thermal properties on the foam's morphology. The cell diameter and porosity of foam are determined together with the thickness of layers for multi-layer thermal insulation, ensuring required operational temperature on the boundaries of layers and a minimum of the total mass of the system.

A wide variety of research papers [2, 3, 10–16, 19–22] presents optimization procedures for the design of multilayer thermal protection systems whose parameters will satisfy formulated constraints and minimize optimization criterion. In most cases, the numerical methods are applied to define the layers' thicknesses, ensuring required operational temperature at the discrete points of the system and the minimum of the total mass.

One of the most popular nonlinear programming methods, widely used to solve the problem under consideration [10, 14], is the penalty function method, which reduces the initial problem of nonlinear function minimization with nonlinear constraints to a sequence of unconstrained minimization problems.

The paper [14] presents an iterative scheme for estimating the thickness of multilayer thermal insulation of the minimum mass with allowance for temperature restrictions for each layer. The problem of unconstrained optimization is solved using the conjugate gradient method for a fixed value of the penalty parameter. The gradient of the penalty function is calculated from the solution of a boundary-value problem adjoint to the initial boundary-value problem, and the step size in the chosen direction is estimated using the sensitivity functions. In [10], the unconstrained minimum of the penalty function is defined using the deformed polyhedron method, which does not require the calculation of the derivatives of the penalty function.

In [16, 19], the optimization problem is solved using genetic algorithms related to evolutionary search methods, which are based on the concepts of genetic inheritance and natural selection, imitating the processes of development of a population of individuals. These algorithms are effective in cases where the objective function is discontinuous, non-differentiable, or strongly nonlinear.

In [22], the optimization procedure is based on the globally convergent method of moving asymptotes [21], which requires the calculation of the gradients of the objective and constraint functions.

In [15], the algorithm for the optimal design of multilayer thermal protection is based on a sequential quadratic programming (SQP) method. The desired parameter vector is defined as the solution of the linearly constrained subproblem with the objective function based on the Lagrangian function. The linear constraints are chosen so that the space of minimization would be restricted within

the subspace of vectors orthogonal to the active constraints' gradients. The Lagrangian function is projected into the reduced subspace of vectors that satisfy the constraints.

The widely used penalty function method has several advantages over other optimization methods. The region in which iterates converge to a solution for this method substantially exceeds the convergence region of other methods, and the algorithms that implement this method are extremely simple. However, the method turns out to be unacceptable for solving optimization problems with high accuracy. Difficulties arise if a too large value of the penalty parameter is chosen, since this makes the optimization problem ill-conditioned.

The penalty function method is especially effective for estimation of initial approximation of the solution, which could be then improved using a method that exhibits good local convergence properties. In this work, the optimization problem is solved using a two-phase computational scheme, which combines the projected Lagrangian method with the quadratic subproblem and the penalty function method. The penalty function method provides a good initial estimate of the optimal parameters vector for the projected Lagrangian method with excellent local convergence properties.

2. OPTIMAL DESIGN

The traditional thermal design problem statement implies determining layers' thickness for multi-layer thermal insulation, ensuring required operational temperature on the boundaries of layers and minimum of the total mass of the system. In this work, the cell diameter and porosity, that characterize the material's morphology, are chosen along with the thicknesses of the layers in order to obtain an additional weight advantage of thermal insulation.

The optimal design problem of multi-layer thermal insulation is considered, assuming that a system consists of L layers made of different materials with density ρ_l , $l = 1, 2, \dots, L$ and thickness d_l , where the layer n is manufactured of a high-porous cellular material. It is assumed that layers $l \neq n$ are opaque and layer n is semitransparent.

The density of the porous layer is expressed through the density ρ_s of the base material, forming the foam, and porosity δ :

$$\rho_n = (1 - \delta) \rho_s.$$

In general case, only the thickness of l_k -th layers $k = 1, 2, \dots, N$, $N \leq L$, is desired. The thickness of the rest of the layers can be assigned proceeding from technological and strength considerations. The design parameters vector \mathbf{p} includes the thickness of layers $k = 1, 2, \dots, N$, $N \leq L$, porosity δ and cell diameter a of the highly porous cellular material, forming layer n .

The criterion for estimation of the design parameters vector is defined by the local mass functional:

$$J(\mathbf{p}) = \sum_{k=1}^N \rho_k d_k. \quad (1)$$

The best estimates should minimize the functional (1) and satisfy the following constraints:

$$d_k > 0, \quad k = 1, 2, \dots, N, \quad (2)$$

$$a_{\min} \leq a \leq a_{\max}, \quad (3)$$

$$0.85 < \delta \leq \delta_{\max}, \quad (4)$$

$$T(X_l, \tau) \leq T_{\lim}^l, \quad l = 1, 2, \dots, L, \quad \tau \in (\tau_{\min}, \tau_{\max}]. \quad (5)$$

The constraints include simple bounds on the variables (2)–(4) and nonlinear constraints on the maximum allowable temperature at the boundary of layers (5). The upper and lower bounds a_{\min} ,

a_{\max} , δ_{\max} are specified, taking into account the porosity and average cell diameter available for manufactured materials.

It is assumed that heat transfer in multilayer thermal protection is one-dimensional by the spatial coordinate, and a temperature distribution $T_l(x, \tau)$ at the layers $l \neq n$ is covered by the quasi-linear heat conduction, whose coefficients C_l and λ_l are functions of temperature:

$$C_l(T_l) \frac{\partial T_l}{\partial \tau} = \frac{\partial}{\partial x} \left(\lambda_l(T_l) \frac{\partial T_l}{\partial x} \right), \quad (6)$$

$x \in (X_{l-1}, X_l)$, $l \neq n$, $\tau \in (\tau_{\min}, \tau_{\max}]$.

A uniform initial temperature distribution in the system is assumed:

$$T_l(x, \tau_{\min}) = T_{0l}, \quad x \in [X_{l-1}, X_l], \quad l = 1, 2, \dots, L.$$

At both sides of the system, there can be the boundary conditions of the first, second or third kind or the boundary condition taking into account heat flux radiated by the surface of the thermal protection:

$$-B_1 \lambda_1(T_1(X_0, \tau)) \frac{\partial T_1(X_0, \tau)}{\partial x} + F_1 T_1(X_0, \tau) = q_1(\tau), \quad (7)$$

$$-B_2 \lambda_L(T_L(X_L, \tau)) \frac{\partial T_L(X_L, \tau)}{\partial x} + F_2 T_L(X_L, \tau) = q_2(\tau), \quad (8)$$

$$-\lambda_L(T_L) \frac{\partial T_L(X_L, \tau)}{\partial x} = -q_A(\tau) + q_R, \quad (9)$$

where $q_A(\tau)$ is the absorbed heat flux, and $q_R = \varepsilon k_B T^4$ is the heat flux radiated by the heated surface of the thermal protection.

A contact heat transfer between opaque layers is characterized by contact thermal resistances, which are also functions of temperature:

$$\lambda_l(T_l) \frac{\partial T_l(X_l, \tau)}{\partial x} = \lambda_{l+1}(T_{l+1}) \frac{\partial T_{l+1}(X_l, \tau)}{\partial x}, \quad (10)$$

$$-\lambda_l(T_l) R_l(T_l) \frac{\partial T_l(X_l, \tau)}{\partial x} = T_l(X_l, \tau) - T_{l+1}(X_l, \tau), \quad (11)$$

$l = 1, 2, \dots, L - 1$, $\tau \in (\tau_{\min}, \tau_{\max}]$.

Radiative-conductive heat transfer in a porous layer n is described by the equation:

$$C_n \frac{\partial T_n}{\partial \tau} = \frac{\partial}{\partial x} \left(\lambda_n \frac{\partial T_n}{\partial x} \right) - \frac{\partial q_R(x)}{\partial x}. \quad (12)$$

The volumetric heat capacity of the foam is

$$C_n = (1 - \delta) \rho_s c_s. \quad (13)$$

The thermal conductivity of the three-dimensional array of solid struts forming the foam structure in the absence of radiation can be expressed by the following simplified relation:

$$\lambda_n = \frac{1}{3} (1 - \delta) \lambda_s. \quad (14)$$

The coefficient $1/3$ is consistent both with the experimental data [17] and theoretical analysis, which takes into account the average number of struts, oriented in each of the orthogonal x , y , and z directions.

Open-cell foam is commonly considered as semi-transparent media, absorbing, emitting and scattering radiation [1, 4–6, 9, 17]. Heat transfer in such media is described by the radiative transfer equation whose solution requires significant computing resources. In engineering applications such as thermal protection system, it is convenient to approximate radiative flux by the Rosseland equation, applicable for optically thick media whose thickness is not less than several photon mean free paths. This approximation leads to appreciable errors in describing the process near the boundaries since it does not take into account radiation from the boundary surfaces. However, within the optically thick layer, the influence of the boundary effects is negligible, since the radiation from the boundary surfaces does not reach the inner layers. The approximation gives a simple expression for the radiation flux using radiative conductivity:

$$q_R = -k_R \frac{dT}{dx},$$

$$k_R = \frac{16n^2 k_B T^3}{3\beta_R}. \quad (15)$$

The effective index of refraction can be taken as $n = 1$, as the foam porosity is very high ($\sim 97\%$). The effects of absorption and scattering are taken into account through the Rosseland mean extinction coefficient β_R defined by the following relation:

$$\frac{1}{\beta_R} = \int_0^\infty \frac{1}{\beta_\lambda^*} \frac{\partial I_{\lambda b}(T)}{\partial I_b(T)} d\lambda.$$

The spectral extinction coefficient β_λ^* is calculated as follows:

$$\beta_\lambda^* = \alpha_\lambda + \sigma_\lambda^*.$$

To account for anisotropic scattering, a weighted scattering coefficient describing the deviation of the radiation via the asymmetry factor is introduced:

$$\sigma_\lambda^* = \sigma_\lambda \cdot (1 - \langle \cos \theta \rangle_\lambda) \quad \text{with the asymmetry factor} \quad \langle \cos \theta \rangle_\lambda = \frac{1}{2} \int_0^\pi \Phi(\theta) \cos \theta \sin \theta d\theta.$$

The solid struts forming the foam structure are assumed to have random orientation and to be thick enough to be considered as opaque. As it has been assumed in several works [1, 4–6, 9], the phase function is presented by a diffuse scattering phase function of opaque particles, and the diffraction contribution is neglected due to the extremely large values of the diffraction phase function in the forward direction. According to [6], the scattering phase function of the open-cell foam obtained using numerical Monte Carlo methods closely matches the scattering phase function of large convex diffusely reflecting particles oriented randomly. The scattering phase function for such particles is identical to the scattering phase function for large opaque spheres made of the same substance with the same surface properties. Under the assumption of complete and diffuse reflection obeying the Lambert law, the scattering phenomena for large spherical particles is described by the following expression:

$$\Phi(\theta) = \frac{8}{3\pi} (\sin \theta - \theta \cos \theta). \quad (16)$$

For scattering phase function (16), the asymmetry factor is $\langle \cos \theta \rangle \approx -0.4444$.

Since the particles forming the open cell foam are assumed opaque, scattering is limited to the diffuse reflection and, additionally, reflectivity is considered independent of incidence angle, the scattering albedo ω_λ is equal to the reflectivity r_λ [4]: $\omega_\lambda = r_\lambda$.

So, the spectral extinction coefficient adjusted for anisotropic scattering is given by:

$$\beta_{\lambda}^* \approx (1 - r_{\lambda}) \cdot \beta + r_{\lambda} \cdot \beta \cdot (1 + 0.4444),$$

$$\frac{1}{\beta_R} = \frac{1}{\beta} \int_0^{\infty} \frac{1}{(1 + 0.4444\rho_{\lambda})} \frac{\partial I_{\lambda b}(T)}{\partial I_b(T)} d\lambda.$$

In [6], there has been proposed an analytical relation to calculate the extinction coefficient β directly from the knowledge of the geometrical characteristics of the foam structure. The relation has been obtained using Monte Carlo simulations for digitally generated foam structures that closely replicate the microstructure of the real foams and take into account the detailed geometrical characteristics of struts. This equation including the average equivalent diameter a , porosity δ , the ratio of the minimum and maximum strut diameters $t = b_{\min}/b_{\max}$ (see Fig. 1) and normalized curvature k (see Fig. 2) as independent variables are used for estimation of extinction coefficient in the present work:

$$\beta = \frac{2.62\sqrt{1-\delta} [1 + 0.22(1-k)^2] [1 - 0.22(1-t)^2]}{a}.$$

At the boundaries of the porous layer n , the following conditions are fulfilled:

$$-\lambda_{n-1}(T_{n-1}) \frac{\partial T_{n-1}(X_{n-1}, \tau)}{\partial x} = -\lambda_n(T_n) \frac{\partial T_n(X_n, \tau)}{\partial x} + q_R(T_n), \quad (17)$$

$$T_{n-1}(X_{n-1}, \tau) = T_n(X_{n-1}, \tau), \quad (18)$$

$$-\lambda_n(T_n) \frac{\partial T_n(X_n, \tau)}{\partial x} + q_R(T_n) = -\lambda_{n+1}(T_{n+1}) \frac{\partial T_{n+1}(X_{n+1}, \tau)}{\partial x}, \quad (19)$$

$$T_n(X_n, \tau) = T_{n+1}(X_n, \tau). \quad (20)$$

The optimization problem, which consists of minimizing an objective function (1) subject to constraints (2)–(5), is solved using a two-phase algorithm based on the projected Lagrangian method with the quadratic subproblem and the penalty function method. The penalty function method is characterized by a large region of convergence and provides a good initial estimate of the optimal parameters' values for the projected Lagrangian method with excellent local convergence properties.

Since penalty functions, generating infeasible iterates are not appropriate for constraints (2)–(4), it is convenient to use the inverse barrier function [7] as a penalty function, which provides an approximate solution of problem (1)–(5) inside the feasible region. Penalty function has the form:

$$P(\mathbf{p}, r) = J(\mathbf{p}) + r \left(\sum_{k=1}^K \frac{1}{p_k} + \sum_{i=1}^m \frac{1}{T_i(\mathbf{p})} \right), \quad (21)$$

where T_i – temperature constraints on the boundaries of the layers. For the numerical solution, a boundary value problem (6)–(20) is approximated on the finite-difference grid with N_{τ} steps by time. Therefore, the constraints (5) can be represented as:

$$T_i = T_{\text{lim}}^l - T(X_l, \tau_j), \quad l = 1, 2, \dots, L, \quad j = 1, 2, \dots, N_{\tau}.$$

The local minimum of penalty function $P(\mathbf{p}, r)$ for a fixed value of the penalty parameter r is found by the Davidon-Fletcher-Powell method. Initial approximation \mathbf{p}^0 must satisfy all constraints. A feasible initial point is found by minimizing the function $F(\mathbf{p}) = -\sum_{j \in \mathbb{I}} T_j(\mathbf{p})$ subject to constraints $T_j(\mathbf{p})$, $j \notin \mathbb{I}$, where \mathbb{I} – a set of indexes of constraints violated at point p .

An algorithm to find an unconstrained minimum of penalty function (21) is executed until two values of iterative sequence P_k and P_{k+1} will not become such that $|(P_k - P_{k+1})/P_k| < \varepsilon$ and $r_k P_k < \varepsilon$,

where P_k – penalty function, and ε – accuracy with which the problem is solved. The estimation of the solution found with the penalty function method is then improved using the projected Lagrangian method with the quadratic subproblem. The method is effective for minimizing a smooth function and is characterized by excellent local convergence properties.

An algorithm contains a sequence of linearly constrained subproblem whose objective function is related to the Lagrangian function:

$$L(\mathbf{p}, \boldsymbol{\psi}) = J(\mathbf{p}) - \boldsymbol{\psi}^T \mathbf{T}. \quad (22)$$

The constraint vector is:

$$\mathbf{T}(\mathbf{p})^T = \{T_{\text{lim}}^1 - T(X_1, \tau_1), \dots, T_{\text{lim}}^l - T(X_l, \tau_{N\tau})\}. \quad (23)$$

The minimum of the Lagrangian function (22) is reached at the desired optimal point \mathbf{p}^* on the set of vectors orthogonal to the active constraints' gradients at \mathbf{p}^* . The desired solution satisfies the following conditions [7]:

$$1) T_{\text{lim}}^l - T(X_l, \tau_{Nj}) \geq 0, \quad l = 1, 2, \dots, L, \quad j = 1, 2, \dots, N_j; \quad \text{where } \mathbf{T}(\mathbf{p}^*) = 0, \quad (24)$$

$$2) \text{grad } J(\mathbf{p}^*) = \mathbf{A}(\mathbf{p}^*)^T \boldsymbol{\psi}^*, \quad (25)$$

where $\mathbf{A}(\mathbf{p}^*)$ is the Jacobian matrix of constraints evaluated at \mathbf{p}^* ,

$$3) \boldsymbol{\psi}_i^* \geq 0, \quad i = 1, 2, \dots, t, \quad (26)$$

$$4) \text{matrix } \mathbf{Z}(\mathbf{p}^*)^T \mathbf{H}(\mathbf{p}^*, \boldsymbol{\psi}^*) \mathbf{Z}(\mathbf{p}^*) \text{ is a positive definite,} \quad (27)$$

where $\mathbf{H}(\mathbf{p}^*, \boldsymbol{\psi}^*)$ – Hessian matrix of Lagrangian function, and $\mathbf{Z}(\mathbf{p}^*)$ – matrix whose columns compose a basis of the subspace of vectors orthogonal to the rows of the matrix $\mathbf{A}(\mathbf{p}^*)$.

Each next approximation to the optimal parameters vector \mathbf{p}^{i+1} is defined by:

$$\mathbf{p}^{i+1} = \mathbf{p}^i + \gamma^i \mathbf{s}^i.$$

A search direction \mathbf{s}^i is found as the solution of the quadratic subproblem whose objective function is a quadratic approximation to the Lagrangian function, and the constraints define the set of points at which the linear approximation to the nonlinear constraints (23) is equal to zero [7].

The quadratic subproblem is written in the form:

$$\text{Minimize } \Phi_L = \mathbf{g}^T \mathbf{s} + \frac{1}{2} \mathbf{s}^T \mathbf{H} \mathbf{s}$$

$$\text{subject to } \mathbf{A}(\mathbf{p}) \mathbf{s} \leq -\mathbf{T},$$

where Φ_L – quadratic approximation to the Lagrangian function, and $\mathbf{g} = \text{grad } J(\mathbf{p}^*) - \mathbf{A}(\mathbf{p})^T \boldsymbol{\psi}$ – gradient of the Lagrangian.

The linear constraints of the subproblem are obtained by expanding the functions (23) about \mathbf{p} in a Taylor series and neglecting the nonlinear term [7]:

$$\mathbf{T}(\mathbf{p}^*) = \mathbf{T}(\mathbf{p}, X_l, \tau_j) + \mathbf{A}(\mathbf{p})(\mathbf{s}) + o(\|\mathbf{s}\|^2) = 0, \quad \mathbf{s} = \mathbf{p}^* - \mathbf{p}.$$

Thus the linear constraints are chosen so that the space of minimization would be restricted within the subspace of vectors orthogonal to the active constraints' gradients.

The Jacobian matrix of the first derivatives of constraints $\mathbf{A}(\mathbf{p})$ is estimated using the sensitivity functions.

The vector optimal for the quadratic subproblem is expressed through the matrices \mathbf{Y} and \mathbf{Z} . Columns of \mathbf{Y} are the elements of matrix $\mathbf{A}(\mathbf{p})$ rows' subspace, and columns of \mathbf{Z} compose a basis for a vector subspace which is orthogonal to the subspace of $\mathbf{A}(\mathbf{p})$ rows:

$$\mathbf{s} = \mathbf{Y} \mathbf{s}_y + \mathbf{Z} \mathbf{s}_z.$$

The feasible vector \mathbf{s} satisfies the equations:

$$\mathbf{A}\mathbf{Y}\mathbf{s}_y = -\mathbf{T}. \quad (28)$$

The vector \mathbf{s}_y , determined by the constraints (28), will be the same for all feasible vectors, and they will differ only in components whose values are not constrained. The vector \mathbf{s}_z is determined by unconstrained minimization of the quadratic approximation of the Lagrange function Φ_L and solves the linear system:

$$\mathbf{Z}^T \mathbf{H}\mathbf{Z}\mathbf{s}_z = -\mathbf{Z}^T (\mathbf{g} + \mathbf{H}\mathbf{Y}\mathbf{s}_y). \quad (29)$$

The next approximation of the vector of Lagrange multipliers is determined from the equation

$$\mathbf{H}\mathbf{s} + \mathbf{g} = \mathbf{A}^T \boldsymbol{\psi}. \quad (30)$$

Once the search direction is found, a step length γ^i is determined by minimizing the augmented Lagrangian merit function [7] written in the form:

$$L_A(\mathbf{p}, \boldsymbol{\psi}, r) = J(\mathbf{p}) - \psi^T \mathbf{T}(\mathbf{p}) + \frac{r}{2} \mathbf{T}(\mathbf{p})^T \mathbf{T}(\mathbf{p}), \quad (31)$$

where r is a penalty parameter that ensures the realization of an unconstrained minimum at a stationary point, found from a sufficient condition for optimality (24)–(27).

A positive-definite approximation to the Hessian of the Lagrangian function is defined by:

$$\mathbf{H}(\tilde{\mathbf{p}}) = \mathbf{H}(\mathbf{p}) - \frac{1}{\mathbf{s}^T \mathbf{H}(\mathbf{p}) \mathbf{s}} \mathbf{H}(\mathbf{p}) \mathbf{s} \mathbf{s}^T \mathbf{H}(\mathbf{p}) + \frac{1}{\mathbf{y}^T \mathbf{s}} \mathbf{y} \mathbf{y}^T, \quad (32)$$

where $\mathbf{y} = \mathbf{g}(\tilde{\mathbf{p}}) - \mathbf{A}(\tilde{\mathbf{p}})^T \boldsymbol{\psi}^* - \mathbf{g}(\mathbf{p})^T + \mathbf{A}(\mathbf{p})^T \boldsymbol{\psi}^*$, $\mathbf{s} = \tilde{\mathbf{p}} - \mathbf{p}$.

The estimated design parameter vector is considered optimal if the following conditions are satisfied:

$$\frac{\gamma \|\mathbf{s}\|}{(1 + \|\mathbf{p}\|)} \leq \varepsilon, \quad (33)$$

$$\frac{\|\mathbf{Z}^T \mathbf{g}\|}{(1 + \max(1 + |J(\mathbf{p})|, \|\mathbf{g}_F(\mathbf{p})\|))} \leq \varepsilon, \quad (34)$$

$$|T_j| \leq \varepsilon_c, \quad (35)$$

where ε is a given positive constant which defines the accuracy of optimization problem solution, ε_c is the maximum acceptable absolute violation in nonlinear constraints, and $\mathbf{g}_F(\mathbf{p})$ is a vector composed of the components of Lagrangian function gradient corresponding to the free variables.

3. DESIGN OF MULTILAYER THERMAL PROTECTION OF SPACECRAFT

To test the efficiency of the developed algorithm and illustrate its capabilities, a problem of design of the thermal protection coating for a re-entry space vehicle descending in the Earth's atmosphere is considered. Coating includes four layers of different materials (see Fig. 3) and is located on the load-bearing structure layer of the spacecraft, made of aluminum alloy ($\lambda = 92.6 \text{ W}/(\text{m} \cdot \text{K})$, $c = 1.006 \text{ kJ}/(\text{kg} \cdot \text{K})$, $\rho = 2640 \text{ kg}/\text{m}^3$) with a thickness $d_1 = 2.5 \text{ mm}$. A layer 2 made of vitreous carbon foam is covered with a layer 3 of the carbon/carbon material with a thickness of $d_3 = 1 \text{ mm}$. Layer 4 is made of silicon carbide foam, and layer 5 is silicon carbide ($d_5 = 2 \text{ mm}$).

It is assumed that the thicknesses of layers 1, 3 and 5 are assigned proceeding from strength or technological requirements. The external heat flux to the re-entry vehicle surface varies according to the dependency shown in Fig. 4.

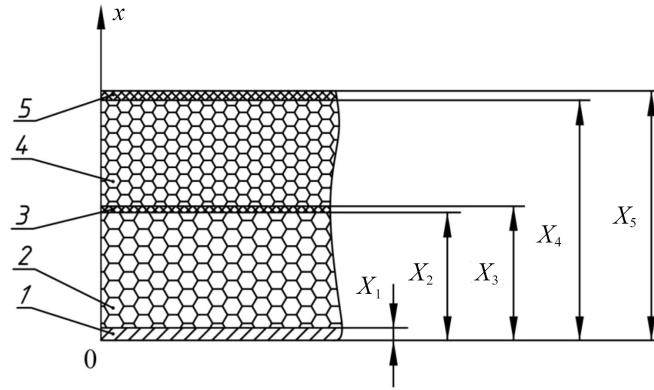


Fig. 3. The scheme of the multilayer thermal protection coating: 1 – aluminum alloy, 2 – vitreous carbon foam, 3 – carbon/carbon, 4 – silicon carbide foam, 5 – silicon carbide.

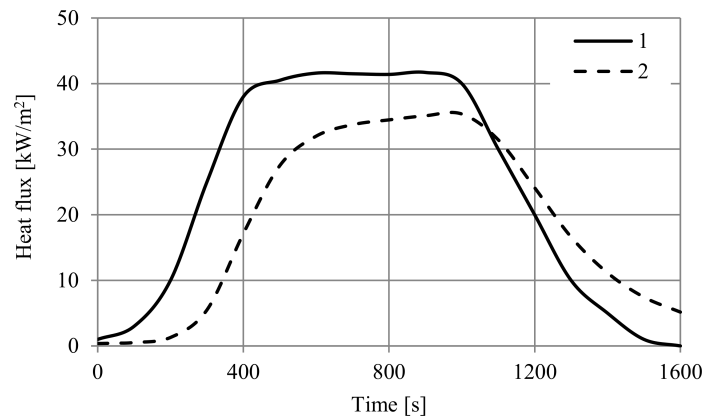


Fig. 4. The external heat flux to the re-entry vehicle surface: 1 – convective heat flux, 2 – heat flux radiated by a surface of the vehicle.

The emissivity of the coating surface is equal to 0.92. The back surface of the multilayer thermal protection coating was assumed thermally insulated. Thermal properties of carbon/carbon, silicon carbide and vitreous carbon forming the highly porous structure of foam used in the simulation are presented in Table 1 [8]. Solid surface reflectivity for silicon carbide and carbon used in calculations is given in Table 2 [8, 18].

Table 1. Thermal properties of materials.

Material	Density [kg/m ³]	Thermal conductivity [W/(m·K)] at temperature [K]			Volumetric heat capacity (10 ³) [J/(m ³ ·K)] at temperature [K]		
		300	500	700	300	500	700
Carbon/carbon	1440	4.91	6.96	7.22	981	1771	2184
Silicon carbide	3200	31	26	21	2144	2898	3379
Vitreous carbon	1800	3.5	5	7	1224	2091	2567

Table 2. The reflectivity of materials as a function of wavelength.

Material	Reflectivity at wavelength [μm]					
	0.5	1	3.5	10	12	35
Carbon	0.325	0.425	0.55	0.75	0.77	0.85
Silicon carbide	0.16	0.16	0.12	0.03	0.99	0.26

The design parameters vector includes thicknesses of layers 2 (d_2) and 4 (d_4), porosity (δ_2 and δ_4), and cell diameters (a_2 and a_4) of the high-porous cellular materials, forming layers 2 and 4.

The maximum work temperature in air for vitreous carbon is 623 K, and for silicon carbide it is 1943 K. Thus, as constraints on maximum allowable temperature, it reasonable to set maximum allowable temperatures at the boundaries of layer 2 made of vitreous carbon foam to 300 K at the inner and 623 K at the outer boundaries with coordinates X_1 and X_2 respectively.

The upper and lower bounds for the variables characterizing the structure of the highly porous materials were set taking into account information about vitreous carbon foams and silicon carbide foams provided by the industry. The porosity of vitreous carbon foams can reach the values of 0.85–0.98. The maximum porosity of silicon carbide foam can be equal to 0.95. The average cell diameter can be in the range of 0.36–5.08 mm, which corresponds to materials with a number of pores per linear inch of 100–10.

A uniform initial temperature distribution in the system is assumed, the temperature is 290 K.

The duration of the heat transfer process for solving the boundary value problem (6)–(20) is 1600 s. The number of steps by time of the finite-difference grid is 2500, and the number of steps by a spatial coordinate in layers 1–5 is 20, 100, 20, 100, 50 respectively.

The accuracy of solving the boundary value problem (6)–(20), the fulfillment of constraints, and the solution of the optimization problem (1)–(5) have been set equal to 10^{-5} . The initial approximations of the desired parameters have been taken as follows: the thickness of the layers 2 and 4: $d_2 = 0.1$ m and $d_4 = 0.1$ m, the porosity of the silicon carbide foam $\delta_4 = 0.9$, and porosity of vitreous carbon foam $\delta_2 = 0.95$. The initial value of the minimized function is 47.89 kg.

The estimated parameters are $d_2 = 0.061$ m, $d_4 = 0.0765$ m, $\delta_2 = 0.98$, $\delta_4 = 0.95$, $a_2 = a_4 = 0.36$ mm. The obtained local mass of the coating is 22.046 kg. Figure 5 shows the time dependences of temperature at the boundaries of the layers.

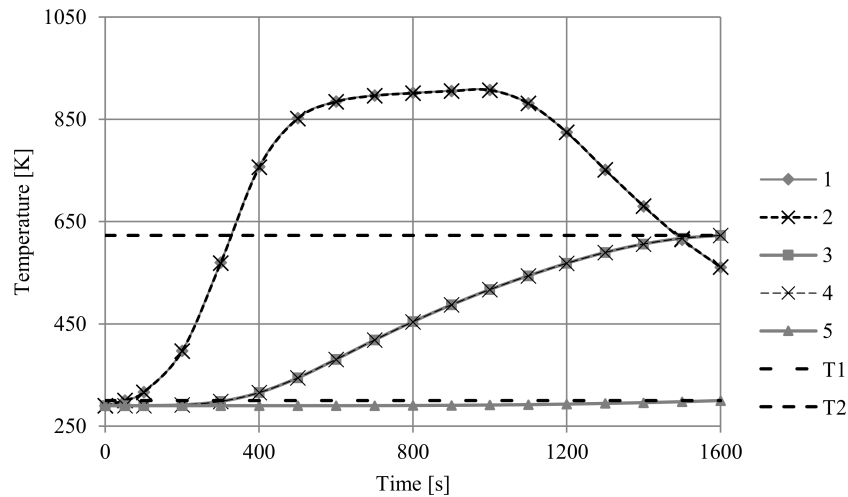


Fig. 5. Time dependence of temperature at the boundaries of the layers: 1 – $T(X_5)$, 2 – $T(X_4)$, 3 – $T(X_3)$, 4 – $T(X_2)$, 5 – $T(X_1)$, T1 – maximum allowable temperature at the boundary of layers with the coordinate X_1 , T2 – maximum allowable temperature at the boundary of layers with the coordinate X_2 .

The number of iterations for minimizing the augmented Lagrangian merit function is equal to 61. The number of iterations required for the solution of the quadratic subproblem is 104 at the beginning of the iteration process and decreases to 1 in the later iterations since the correct active constraints have been identified near the solution. The cumulative number of evaluation of the objective function needed for the line search is 272.

The optimal porosity of vitreous carbon foam and silicon carbide foam is equal to the upper bound, and the optimal cell diameters of these materials are equal to the lower bound set for these variables. These results agree with the theoretical model of heat transfer in the porous layers underlying the developed algorithm. According to the relations used to calculate the radiative

component of thermal conductivity, materials with the minimum cell diameter have the best thermal insulation properties. The obtained results confirm the correctness and effectiveness of the developed algorithm for the optimal design of multilayer thermal protection, taking into account the foam morphology.

4. CONCLUSION

A new method has been developed for choosing optimal parameters for multilayer thermal protection based on highly porous cellular materials. The porosity and cell diameter of foam are included in the parameters' vector and may be chosen along with the thicknesses of layers. The traditional techniques for the design of multilayer thermal protection suggest the availability of thermal properties of all materials composing the layers as initial data for the design problem. The required information, in this case, could be obtained through the thermal tests of the materials' samples or simulations. The proposed algorithm allows choosing the porosity and cell diameter of a layer made of open-cell foam without fabrication and experimental research of samples or simulation of their thermal properties, and, therefore reducing the amount of preliminary research in designing of thermal protection. The constructed algorithm is applicable without modification for solving a wide range of thermal design problems, including the design of advanced thermal protection systems for spacecraft operating under conditions of extreme thermal loads.

ACKNOWLEDGEMENTS

This work was supported by the Russian Science Foundation (Grant no. 18-19-00492).

REFERENCES

- [1] D. Baillis, M. Raynaud, J.F. Sacadura. Determination of spectral radiative properties of open cell foam: Model validation. *Journal of Thermophysics and Heat Transfer*, **14**(2): 137–143, 2000, doi: 10.2514/2.6519.
- [2] A. Yu. Bushuev, V.V. Gorskii. One approach to constructing a method for designing model heat shields. *Journal of Engineering Physics*, **61**(3): 1150–1156, 1991, doi: 10.1007/BF00872896.
- [3] A. Yu. Bushuev, V.V. Gorskii. Use of sensitivity functions in the problem of designing a multilayer heat shield. *Journal of Engineering Physics*, **61**(6): 1548–1554, 1991, doi: 10.1007/BF00872013.
- [4] R. Coquard, D. Rochais, D. Baillis. Conductive and radiative heat transfer in ceramic and metal foams at fire temperatures. *Fire Technology*, **48**(3): 699–732, 2012, doi: 10.1007/s10694-010-0167-8.
- [5] S. Cunsolo, R. Coquard, D. Baillis, N. Bianco. Radiative properties modeling of open cell solid foam: Review and new analytical law. *International Journal of Thermal Sciences*, **104**: 122–134, 2016, doi: 10.1016/j.ijts.2016.05.007.
- [6] S. Cunsolo, R. Coquard, D. Baillis, W.K.S. Chiu, N. Bianco. Radiative properties of irregular open cell solid foams. *International Journal of Thermal Sciences*, **117**: 77–89, 2017, doi: 10.1016/j.ijthermalsci.2017.03.007.
- [7] P.E. Gill, W. Murray, M.H. Wright. *Practical Optimization*. Academic Press, London, 1981.
- [8] I.S. Grigoriev, E.Z. Meilikhov [Eds]. *Physical Quantities: Directory* [in Russian]. Energoatomizdat, Moscow, 1991.
- [9] M. Loretz, R. Coquard, D. Baillis, E. Maire. Metallic foams: Radiative properties/comparison between different models. *Journal of Quantitative Spectroscopy and Radiative Transfer*, **109**(1): 16–27, 2008, doi: 10.1016/j.jqsrt.2007.05.007.
- [10] I.A. Maiorova, P.V. Prosuntsov, A.V. Zuev. Optimal thermal design of a multishield thermal protection system of a reusable space vehicles. *Journal of Engineering Physics and Thermophysics*, **89**(2): 528–533, 2016, doi: 10.1007/s10891-016-1406-8.
- [11] R.A. Meric. Finite element analysis of optimal heating of a slab with temperature-dependent thermal conductivity. *International Journal Heat and Mass Transfer*, **22**(10): 1347–1353, 1978, doi: 10.1016/0017-9310(79)90197-2.
- [12] R.A. Meric. Optimal thermal insulation by the boundary element method. *Numerical Heat Transfer*, **9**(2): 163–182, 1986.
- [13] R.A. Meric. Sensitivity analysis and optimization for Joule heating with temperature-dependent conductivities. *Numerical Heat Transfer. Part B: Fundamentals*, **16**(2): 213–229, 1990, doi: 10.1080/10407798908944936.

- [14] V.V. Mikhailov. Optimization of multilayer thermal insulation. *Journal of Engineering Physics*, **39**(2): 880–884, 1980.
- [15] A.V. Nenarokomov. Design of a system of multilayer heat insulation of minimum mass [in Russian]. *TVT*, **35**(6): 909–916; *High Temperature*, **35**(6): 896–903, 1997.
- [16] M. Nosratollahi, M. Mortazavi, A. Adami, M. Hosseini. Multidisciplinary design optimization of a reentry vehicle using genetic algorithm. *Aircraft Engineering and Aerospace Technology: An International Journal*, **82**(3): 194–203, 2010, doi: 10.1108/00 022661011075928.
- [17] A. Öchsner, G.E. Murch, M.J.S. de Lemos [Eds]. *Cellular and Porous Materials: Thermal Properties Simulation and Prediction*. Wiley-VCH, Weinheim, 2008.
- [18] R.J. Papoular, R. Papoular. Some optical properties of graphite from IR to millimetric wavelengths. *Monthly Notices of the Royal Astronomical Society*, **443**(4): 2974–2982, 2014, doi: 10.1093/mnras/stu1348.
- [19] A. Riccio, F. Raimondo, A. Sellitto, V. Carandente, R. Scigliano, D. Tescione. Optimum design of ablative thermal protection systems for atmospheric entry vehicles. *Applied Thermal Engineering*, **119**: 541–552, 2017, doi: 10.1016/j.applthermaleng.2017.03.053.
- [20] A.A. Shmukin, R.A. Posudievskii. Optimization of multilayer fusing heat-insulating coating. *Journal of Engineering Physics*, **50**(2): 174–178, 1986, doi: 10.1007/BF00870083.
- [21] K. Svanberg. The method of moving asymptotes – a new method for structural optimization. *International Journal for Numerical Methods of Engineering*, **24**(2): 359–373, 1987, doi: 10.1002/nme.1620240207.
- [22] G. Xie, Q. Wang, B. Sunden, W. Zhang. Thermomechanical optimization of lightweight thermal protection system under aerodynamic heating. *Applied Thermal Engineering*, **59**(1–2): 425–434, 2013, doi: 10.1016/j.applthermaleng.2013.06.002.